

Original Research Article

Alleviating glucose repression and enhancing respiratory capacity to increase itaconic acid production

Yaying Xu^a, Zhimin Li^{a,b,*}^a State Key Laboratory of Bioreactor Engineering, East China University of Science and Technology, 130 Meilong Road, Shanghai, 200237, China^b Shanghai Collaborative Innovation Center for Biomufacturing Technology, 130 Meilong Road, Shanghai, 200237, China

ARTICLE INFO

Keywords:

Itaconic acid
Glucose repression
Signaling pathway

ABSTRACT

The Crabtree effect products ethanol and acetic acid can be used for itaconic acid (IA) production in *Saccharomyces cerevisiae*. However, both the IA synthesis and oxidative phosphorylation pathways were hampered by glucose repression when glucose was used as the substrate. This study aimed to improve IA titer by increasing gene expressions related to glucose derepression without impairing yeast growth on glucose. Engineering the acetyl-CoA synthesis pathway increased the titer of IA to 257 mg/L in a urea-based medium. Instead of entire pathway overexpression, we found that some signaling pathways regulating glucose repression were effective targets to improve IA production and respiratory capacity. As a consequence of the reduced inhibition, IA titer was further increased by knocking out a negative regulator of the mitochondrial retrograde signaling MKS1. SNF1/MIG1 signaling was disturbed by deleting the hexokinase HXK2 or an endoplasmic reticulum membrane protein GSF2. The shaking results showed that XYY286 (BY4741, HO::*cadA*, Y::*Dz.ada*, 208a::*Mt.acs*, Δ *hxc2*, pRS415-*cadA*, pRS423-*aac2*) accumulated 535 mg/L IA in 168 h in the YSCGLU medium. qRT-PCR results verified that deletion of MKS1 or HXK2 upregulated the gene expressions of the IA synthesis and respiratory pathways during the growth on glucose.

1. Introduction

Itaconic acid (IA) is a five-carbon unsaturated binary organic acid consisting of two carboxyl groups and one vinyl group. Its trifunctional structure enables IA to be synthesized into various novel biopolymers, widely used in food and biomedical and other industries [1–3]. *Aspergillus terreus* fermentation is the primary method used in industry for IA production and has been widely employed domestically and internationally for a long time [4]. IA is derived naturally from citric acid catalyzed by the *cis*-aconitic acid decarboxylase (CADA), a pathway that has been successfully expressed in most industrial microorganisms, such as *Aspergillus niger*, *Escherichia coli*, *Ustilago maydis*, and others [5–8]. As a phage-resistant and acid-tolerant platform, *Saccharomyces cerevisiae* is crucial to producing organic acids because it is both safe for biological use and easy to modify genetically. *S. cerevisiae* has been used as a platform for IA bioproduction by creating an IA production pathway in

the cytoplasm [9,10].

Previously [11], we reported that during the ethanol-acetic acid utilization stage of *S. cerevisiae* citric acid could be provided via the glyoxylate pathway and TCA cycle without creating an IA production pathway (Fig. 1). Recent research has also inferred that *S. cerevisiae* can use ethanol to generate acetyl-CoA for the mitochondrial TCA cycle and cytoplasmic fatty acid synthesis with the isotope labeling method. Additionally, cells can absorb ethanol as a crucial source of NADPH [12]. The ethanol utilization can provide both a carbon source and energy for IA production. However, ethanol and acetic acid was metabolized slowly and affected cell growth. Although *S. cerevisiae* grew quickly on glucose, glucose repression inhibited the IA synthesis pathway. We designed an IA biosynthetic system that grew exceptionally on glucose and produced IA on ethanol and acetate mostly. Reducing the inhibition of IA synthesis and ATP supply during glucose utilization helps to alleviate the pressure of IA synthesis with ethanol. As a primary source of

Abbreviations: YSCGL, YSC medium with ammonium sulfate and glucose as substrates; YSCGLU, YSC medium with urea and glucose as substrates; YPD, Yeast extract peptone dextrose; IA, Itaconic acid.

Peer review under responsibility of KeAi Communications Co., Ltd.

* Corresponding author. State Key Laboratory of Bioreactor Engineering, East China University of Science and Technology, 130 Meilong Road, Shanghai, 200237, China.

E-mail address: lizm@ecust.edu.cn (Z. Li).

<https://doi.org/10.1016/j.synbio.2022.12.007>

Received 13 October 2022; Received in revised form 8 December 2022; Accepted 21 December 2022

Available online 24 December 2022

2405-805X/© 2022 The Authors. Publishing services by Elsevier B.V. on behalf of KeAi Communications Co. Ltd. This is an open access article under the CC BY-NC-ND license (<http://creativecommons.org/licenses/by-nc-nd/4.0/>).

Table 1
Strains and plasmids used in this study.

Name	Genotype	Source or reference
strains		
BY4741	MATa; his3Δ1; leu2Δ0; met15Δ0; ura3Δ0	
xyy270	BY4741, HO::P _{GPD} - <i>cadA</i> -T _{CYC1}	This study
xyy271	xyy270, YPRCd15c ^a ::P _{GPD} - <i>Dz.ada</i> -T _{CYC1}	This study
xyy272	xyy271, 308a::P _{TEF1} - <i>adh2</i> -T _{CYC1}	This study
xyy273	xyy270, 208a::P _{TEF1} - <i>Ec.ackA</i> -T _{CYC1} , 720a::P _{Fba1} - <i>Ec.pta</i> -T _{CYC1}	This study
xyy274	xyy271, 208a::P _{TEF1} - <i>Ec.ackA</i> -T _{CYC1} , 720a::P _{Fba1} - <i>Ec.pta</i> -T _{CYC1}	This study
xyy275	xyy272, 208a::P _{TEF1} - <i>Ec.ackA</i> -T _{CYC1} , 720a::P _{Fba1} - <i>Ec.pta</i> -T _{CYC1}	This study
xyy276	xyy270, 208a::P _{GPD} - <i>Mt.acs</i> -T _{CYC1}	This study
xyy277	xyy271, 208a::P _{GPD} - <i>Mt.acs</i> -T _{CYC1}	This study
xyy278	xyy272, 208a::P _{GPD} - <i>Mt.acs</i> -T _{CYC1}	This study
xyy282	xyy270, Δ <i>mks1</i>	This study
xyy283	xyy271, Δ <i>mks1</i>	This study
xyy284	xyy277, Δ <i>mks1</i>	This study
xyy286	xyy277, Δ <i>hvk2</i>	This study
xyy288	xyy284, Δ <i>hvk2</i>	This study
xyy290	xyy277, Δ <i>gsf2</i>	This study
xyy292	xyy284, Δ <i>gsf2</i>	This study
XY270	pRS415-P _{GPD} - <i>cadA</i> -T _{CYC1} , pRS423-P _{TEF1} - <i>aac2</i> -T _{CYC1}	This study
XY271	xyy271, pRS415-P _{GPD} - <i>cadA</i> -T _{CYC1} , pRS423-P _{TEF1} - <i>aac2</i> -T _{CYC1}	This study
XY272	xyy272, pRS415-P _{GPD} - <i>cadA</i> -T _{CYC1} , pRS423-P _{TEF1} - <i>aac2</i> -T _{CYC1}	This study
XY273	xyy273, pRS415-P _{GPD} - <i>cadA</i> -T _{CYC1} , pRS423-P _{TEF1} - <i>aac2</i> -T _{CYC1}	This study
XY274	xyy274, pRS415-P _{GPD} - <i>cadA</i> -T _{CYC1} , pRS423-P _{TEF1} - <i>aac2</i> -T _{CYC1}	This study
XY275	xyy275, pRS415-P _{GPD} - <i>cadA</i> -T _{CYC1} , pRS423-P _{TEF1} - <i>aac2</i> -T _{CYC1}	This study
XY276	xyy276, pRS415-P _{GPD} - <i>cadA</i> -T _{CYC1} , pRS423-P _{TEF1} - <i>aac2</i> -T _{CYC1}	This study
XY277	xyy277, pRS415-P _{GPD} - <i>cadA</i> -T _{CYC1} , pRS423-P _{TEF1} - <i>aac2</i> -T _{CYC1}	This study
XY278	xyy278, pRS415-P _{GPD} - <i>cadA</i> -T _{CYC1} , pRS423-P _{TEF1} - <i>aac2</i> -T _{CYC1}	This study
XY282	xyy282, pRS415-P _{GPD} - <i>cadA</i> -T _{CYC1} , pRS423-P _{TEF1} - <i>aac2</i> -T _{CYC1}	This study
XY283	xyy283, pRS415-P _{GPD} - <i>cadA</i> -T _{CYC1} , pRS423-P _{TEF1} - <i>aac2</i> -T _{CYC1}	This study
XY284	xyy284, pRS415-P _{GPD} - <i>cadA</i> -T _{CYC1} , pRS423-P _{TEF1} - <i>aac2</i> -T _{CYC1}	This study
XY286	xyy286, pRS415-P _{GPD} - <i>cadA</i> -T _{CYC1} , pRS423-P _{TEF1} - <i>aac2</i> -T _{CYC1}	This study
XY288	xyy288, pRS415-P _{GPD} - <i>cadA</i> -T _{CYC1} , pRS423-P _{TEF1} - <i>aac2</i> -T _{CYC1}	This study
XY290	xyy290, pRS415-P _{GPD} - <i>cadA</i> -T _{CYC1} , pRS423-P _{TEF1} - <i>aac2</i> -T _{CYC1}	This study
XY292	xyy292, pRS415-P _{GPD} - <i>cadA</i> -T _{CYC1} , pRS423-P _{TEF1} - <i>aac2</i> -T _{CYC1}	This study
Plasmids		
	Characteristic(s)	Reference
pRS415-P _{GPD} - <i>cadA</i> -T _{CYC1}	<i>cadA</i> expression plasmid	This study
pRS423-P _{TEF1} - <i>aac2</i> -T _{CYC1}	<i>aac2</i> expression plasmid	This study
pRS426-P _{GPD} - <i>Dz.ada</i> -T _{CYC1}	<i>Dz.ada</i> expression plasmid	This study
pRS423-P _{TEF1} - <i>adh2</i> -T _{CYC1}	<i>adh2</i> expression plasmid	This study
pRS423-P _{TEF1} - <i>Ec.ackA</i> -T _{CYC1}	<i>Ec.ackA</i> expression plasmid	This study
pRS423-P _{Fba1} - <i>Ec.pta</i> -T _{CYC1}	<i>Ec.pta</i> expression plasmid	This study
pRS426-P _{GPD} - <i>Mt.acs</i> -T _{CYC1}	<i>Mt.acs</i> expression plasmid	This study
pPOX-gRNA-Y	gRNA cassette	This study
pHYB-gRNA-308a	gRNA cassette	This study
pHYB-gRNA-208a	gRNA cassette	This study
pHYB-gRNA-720a	gRNA cassette	This study
pHYB-gRNA-mks1	gRNA cassette	This study
pPOX-gRNA-hvk2	gRNA cassette	This study
pPOX-gRNA-gsf2	gRNA cassette	This study

^a YPRCd15c was noted as Y in the manuscript.

optimized and synthesized by Genewiz (GenBank: CP000477.1) and inserted into pRS426-P_{GPD}-T_{CYC1}, yielding plasmid pRS426-P_{GPD}-*Mt.acs*-T_{CYC1}. Gene deletion and integration on the chromosome were performed using a CRISPR/Cas9-mediated method, as previously reported [11,24]. Yeast transformation was performed using a Frozen EZ Yeast Transformation II Kit (Zymo Research, USA). *S. cerevisiae* BY4741 was used as chassis cell. Strain xyy270 was constructed by inserting P_{GPD}-*cadA*-T_{CYC1} cassette into integration position HO characterized in a previous study [25]. The linear integration cassettes P_{GPD}-*Dz.ada*-T_{CYC1}, P_{TEF1}-*adh2*-T_{CYC1}, P_{TEF1}-*Ec.ackA*-T_{CYC1}, P_{Fba1}-*Ec.pta*-T_{CYC1} and P_{GPD}-*Mt.acs*-T_{CYC1} were inserted into integration positions characterized in a previous study [26]. More details about the constructed strains are listed in Table 1. A map of the strain evolution was supplemented in Fig. S1.

2.2. Medium and cultivation conditions

E. coli strains were grown in Luria-Bertani medium (1% (w/v) tryptone, 0.5% (w/v) yeast extract, and 1% (w/v) NaCl) at 37 °C

supplemented with 100 mg/L ampicillin. Solid LB medium contained 2.0% Bacto agar. Yeast strains were cultivated in yeast extract peptone dextrose (YPD) before the transformation. YPD media contained 20 g/L glucose, 20 g/L peptones, and 10 g/L yeast extract. For maintenance, stock cultures of yeast strains were grown on YPD, if not specified differently, and *E. coli* cultures on LB medium with an appropriate antibiotic marker until the late exponential phase, complemented with sterile glycerol to a final concentration of 50% (vol/vol), and stored at –80 °C as 1-ml aliquots until further use.

Aerobic shake-flask cultures were grown in 250-mL shake flasks containing 30 mL of liquid media set at 30 °C and 220 rpm. For fermentation in flasks, the primary preculture cultures were prepared by inoculating strains transferred with plasmids pRS415-P_{GPD}-*cadA*-T_{CYC1} and pRS423-P_{TEF1}-*aac2*-T_{CYC1} on solid medium to 2 mL YSCGL medium containing 20 g/L glucose, 0.67 g/L yeast nitrogen base, a complete supplement mixture (CSM) amino acid dropout supplement, and appropriate amino acids (LEU 0.1 g/L, HIS 0.05 g/L, URA 0.1 g/L and MET 0.05 g/L, according to the auxotroph markers of plasmids). The

nitrogen source of the shake flask medium was changed to 2 g/L urea (except for the shake flask medium in Fig. 2A with 5 g/L ammonium sulfate), which was named YSCGLU in this paper. Cells were harvested by centrifugation at 6000 rpm for 5 min, washed with fresh medium, transferred to a 250 mL flask containing 30 mL of YSCGL or YSCGLU medium, and grown at 30 °C and 220 rpm.

2.3. Analytical methods

Cell growth was monitored by measuring the absorbance at 600 nm. The concentrations of glucose, ethanol, acetate, glycerol, citric acid/isocitric acid, OAA, pyruvic acid and IA were analyzed by HPLC with an Aminex HPX-87H ion exclusion column (Bio-Rad, Hercules, CA), a refractive index detector (RID-10A, Shimadzu Corporation, Kyoto,

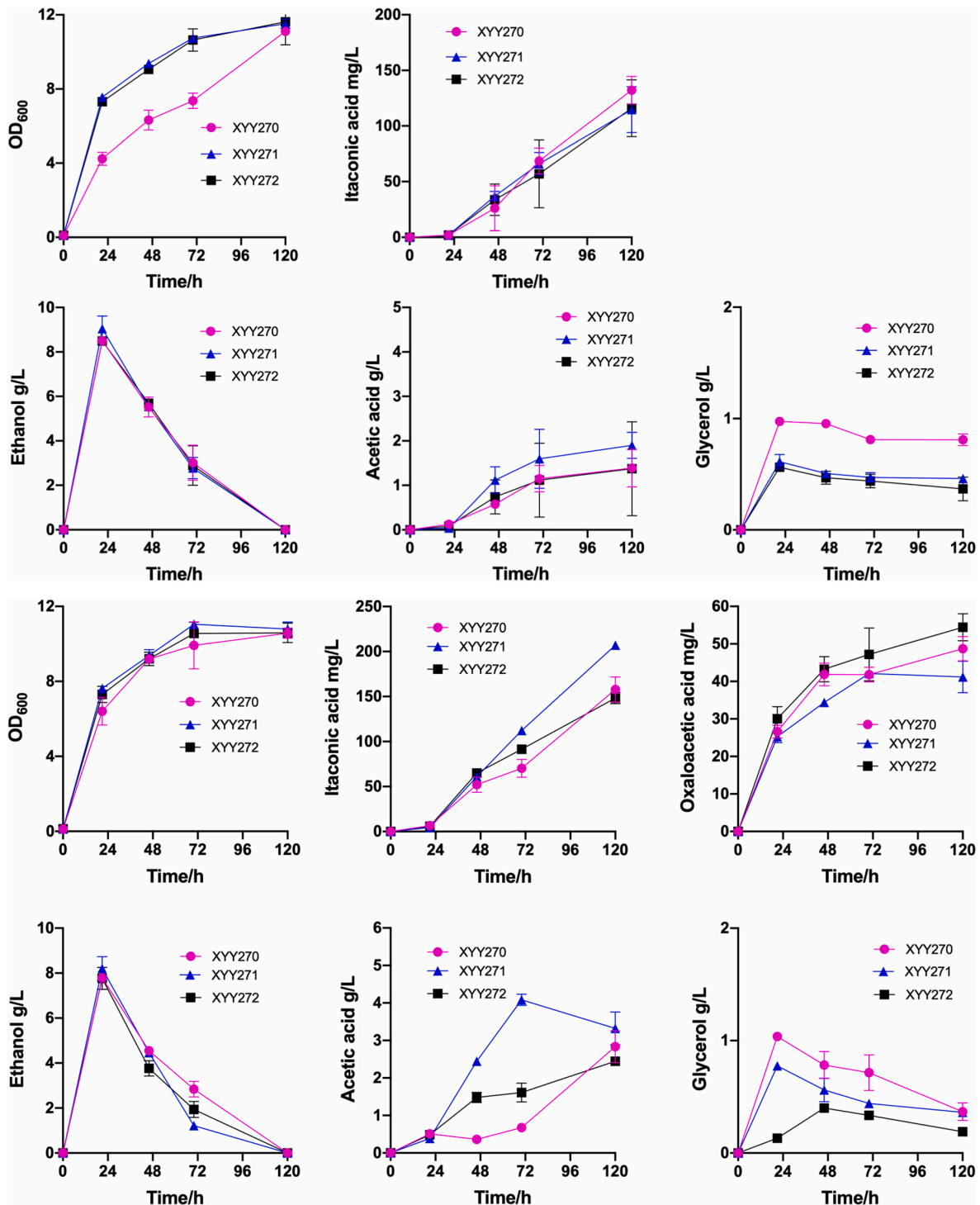


Fig. 2. Effect of enhanced ethanol utilization on IA production and metabolism. (A) Production of IA with 5 g/L ammonium sulfate. (B) Production of IA with 2 g/L urea. XYY270 (●); XYY271 (▲); XYY272 (■). Strain XYY271 overexpressed *Dz.ada*, strain XYY272 overexpressed *Dz.ada* and *Sc.adh2*, and XYY270 was a control strain with plasmids pRS415-*P_{GPD}-cadA-T_{CYC1}* and pRS423-*P_{TEF1}-aac2-T_{CYC1}*. The seed cultures were inoculated into 30 mL of medium with an initial OD₆₀₀ of 0.1 and the pre-cultured cells were harvested at 20 h in YSC medium with 5 g/L ammonium sulfate or 2 g/L urea as nitrogen source. The pH of the medium was adjusted with NaOH or HCl every 24 h to about 6.00.

Japan), a UV detector (SPD-10A, Shimadzu Corporation), and an LC Solutions system (Shimadzu Corporation). IA was measured with the UV detector and the other metabolism were measured with the refractive index detector. The mobile phase was 5 mM H₂SO₄ solution at a flow rate of 0.5 mL/min. The HPLC column was operated at 30 °C. Additionally, profiles of glucose and pyruvic acid concentrations of constructed strains in YSCGL or YSCGLU medium were added in Fig. S2, Fig. S3, Fig. S4 and Fig. S5.

2.4. RNA isolation and quantitative real-time PCR

The primers used for quantitative real-time PCR analysis (qRT-PCR) are listed in Table S1. The yeast culture of shake flask was sampled at 19 h and 48 h, centrifuge at 6000 rpm for 10 min. The collect cells were washed once with PBS (pH = 7.0) or sterile water. Then the cells were frozen with liquid nitrogen, transferred to the mortar, and ground to powder. The RNA was extracted using the SteadyPure Universal RNA Extraction Kit II (Accurate Biotechnology (Hunan)Co., Ltd.) and translated into cDNA using an Evo M-MLVRT Mix Kit (Accurate biology). The RNA quality was analyzed by agarose gel electrophoresis and nanodrop, and 10-fold diluted cDNA was employed as a template to perform qRT-PCR using SYBR® Green Premix Pro Taq HS qPCR Kit (Accurate biology) in the Bio-Rad CFX96 Real-Time PCR system (Bio-Rad). The actin gene (GenBank Gene ID: 850504, ACT1) was used as an internal control for BY4741. The relative abundances of genes: *idh1*, *idh2*, *pyc1*, *acs1*, *cit1*, *cit2*, *aco1* and so on were standardized by the expression levels of the actin gene, and the relative quantification of each transcript was achieved using the 2^{-ΔΔCt} method, as previously reported [27]. The enumerations were performed in triplicate for each group of data, and the average was taken into consideration.

3. Results

3.1. Engineering the ethanol consumption pathway

Ethanol and acetic acid formed because of the Crabtree effect could be used for IA production and overexpression of the ATP/ADP transporter AAC2 increased IA biosynthesis [11]. However, acetic acid accumulated gradually during ethanol utilization (2.5 g/L at 120 h), which had a toxic effect on cell metabolism and inhibited cellular growth. As ethanol was about to be consumed, acetic acid was gradually utilized at a moderate speed. Ethanol higher than 4.25 g/L will prevent acetic acid utilization since a high concentration of ethanol prevents the transcription of ACS1 [28,29]. Increasing ethanol utilization preferentially will help to boost the rate of acetic acid absorption. Acetaldehyde dehydrogenase (acylation) *Dz.ada* [14] from *Dickeya parazeae* Ech586 and ethanol dehydrogenase ADH2 from *S. cerevisiae* S288C were overexpressed, and the cassette P_{GPD}-*Dz.ada*-T_{CYC1} was integrated into the YPRCD15c site of *xyy270* (BY4741, HO:P_{GPD}-*cadA*-T_{CYC1}) to obtain strain *xyy271*. P_{TEF1}-*adh2*-T_{CYC1} expression cassette was integrated into the 308a site of *xyy271* to obtain strain *xyy272*. Plasmids pRS415-P_{GPD}-*cadA*-T_{CYC1} and pRS423-P_{TEF1}-*aac2*-T_{CYC1} were transformed into *xyy270* to obtain *XYy270*. As shown in Table 1, strains named with capital letters contain the two plasmids.

Both *Dz.ada* and *adh2* were overexpressed and the obtained strains were cultured in a YSCGL-LEU-HIS medium with 5 g/L ammonium sulfate as a nitrogen source (Fig. S2A). Fig. 2A showed that it had no significant impact on the production of acetic acid, IA, or ethanol except for raising the biomass of *S. cerevisiae*. However, previous studies had demonstrated that *S. cerevisiae* improved IA yield by simultaneously overexpressing acetaldehyde dehydrogenase (acylation), citrate synthase, and aconitase [9]. We replaced the 5 g/L ammonium sulfate in the medium YSCGL-LEU-HIS with 2 g/L urea (YSCGLU). During the ethanol utilization stage, the ethanol utilization rate of *XYy271* was faster than that of the control strain *XYy270*, acetic acid accumulated gradually, and entered the acetic acid utilization stage earlier than that of the

control strain *XYy270*. After 72 h, the acetic acid utilization started, and the IA titer increased to 207 mg/L in 120 h (Fig. 2B). The IA concentration of *XYy271* improved from 48 h to 120 h mostly, consistent with accelerated ethanol and acetic acid utilization, which reflected strengthened metabolic flux in the ethanol-acetyl-CoA pathway of *XYy271* after 48 h.

3.2. Engineering the acetic acid consumption pathway

Although exogenous expression of *Dz.ada* encouraged IA production and metabolic flux of the ethanol-acetyl-CoA pathway, it still took a long time for acetic acid to be utilized, leaving around 2.08 g/L of acetic acid residue in the 120-h supernatant of *XYy271*. To speed up the utilization of acetic acid further, we overexpressed ACKA-PTA [27] from *Escherichia coli* BW25113 and acetyl-CoA synthase (Mt.ACS) from *Methanotrix thermoacetophila* [30,31], respectively.

Ec.ackA catalyzes acetic acid and ATP into acetyl-phosphate and ADP, and then acetyl-phosphate is converted into acetyl-CoA under the control of *Ec.pta*. Compared with the general reaction of acetyl-CoA synthase, the advantage of ACK-PTA pathway is reducing one ATP demand for acetic acid utilization. However, when the carbon flux entering the cells exceed the digestion capacity of the central pathway and acetyl-CoA cannot enter the TCA cycle pathway, excessive acetyl-CoA could produce acetic acid and ATP through the ACK-PTA pathway reversely [32]. The expression cassettes of P_{TEF1}-*Ec.ackA*-T_{CYC1} and P_{Fba1}-*Ec.pta*-T_{CYC1} were integrated into 208a and 720a of *xyy270*, respectively, yielding strain *xyy273*. P_{TEF1}-*Ec.ackA*-T_{CYC1} and P_{Fba1}-*Ec.pta*-T_{CYC1} expression cassettes were integrated into the same sites of *xyy271* to obtain strain *xyy274*. P_{TEF1}-*Ec.ackA*-T_{CYC1} and P_{Fba1}-*Ec.pta*-T_{CYC1} expression cassettes were integrated into the exact positions of *xyy272* to obtain strain *xyy275*. As shown in Fig. 3A, strains *XYy274* and *XYy275* overexpressing *Ec.ackA* and *Ec.pta* accelerated ethanol utilization after 48 h, but yeast biomass in the utilization stage of ethanol and acetic acid was significantly lower than that of the control strain *XYy270*. Acetic acid concentrations reached 4.74 g/L and 5.51 g/L after 120 h, which was higher than the titer of acetic acid accumulated in *XYy271* (4.08 g/L), the control strain. Accumulation of acetic acid might prevent yeast growth. The production of IA, the downstream product synthesized by acetyl-CoA, was reduced to 77 mg/L and 60 mg/L, respectively. Overexpression of *Ec.ackA* and *Ec.pta* resulted in more excretion of acetic acid and less production of IA at 120 h.

Although acetyl-CoA synthase can catalyze the reaction between acetic acid and acetyl-CoA reversibly, pyrophosphatase makes the activity irreversible in yeast. Acetyl-CoA synthetase from *Methanotrix thermoacetophila* has a Km value of 0.4 mM and a high affinity for acetic acid. Additionally, the enzyme has a higher affinity for ATP than *S. cerevisiae* acetyl-CoA synthetase ACS1. A P_{GPD}-*Mt.acs*-T_{CYC1} expression cassette was integrated at the position 208a of *xyy270* to obtain strain *xyy276*; For strain *xyy277*, the P_{GPD}-*Mt.acs*-T_{CYC1} expression cassette was integrated at the position 208a of *xyy271*; P_{GPD}-*Mt.acs*-T_{CYC1} expression cassette was integrated at the position 208a of *xyy272* to obtain strain *xyy278*.

XYy277 overexpressed *Mt.acs* based on strain *XYy271* and the biomass decreased. The concentration of IA increased to 258 mg/L after 120 h (Fig. 3B). Besides, the concentrations of OAA and pyruvic acid in the supernatant increased significantly. qRT-PCR results showed (Fig. 3C) that the relative expression of *idh2*, *ndi1*, *nde1* and *qcr6* related to mitochondrial respiratory metabolism in strain *XYy277* was up-regulated by 2.0, 5.0, 3.0, 2.3 and 2.7 times than that in strain *XYy271* at 48 h (the stage of ethanol utilization), and the difference was significant. Additionally, the relative expression of the genes in the glyoxylate pathway, *mls1*, *mdh2* and *icl1* were 1.6, 5.0 and 4.3 higher than that of *XYy271*, which was consistent with the increase in OAA production. The relative expression of pyruvate carboxylase *PYC1* did not change significantly, suggesting that the up-regulated expression of the glyoxylate pathway may be the primary cause of the rise in OAA

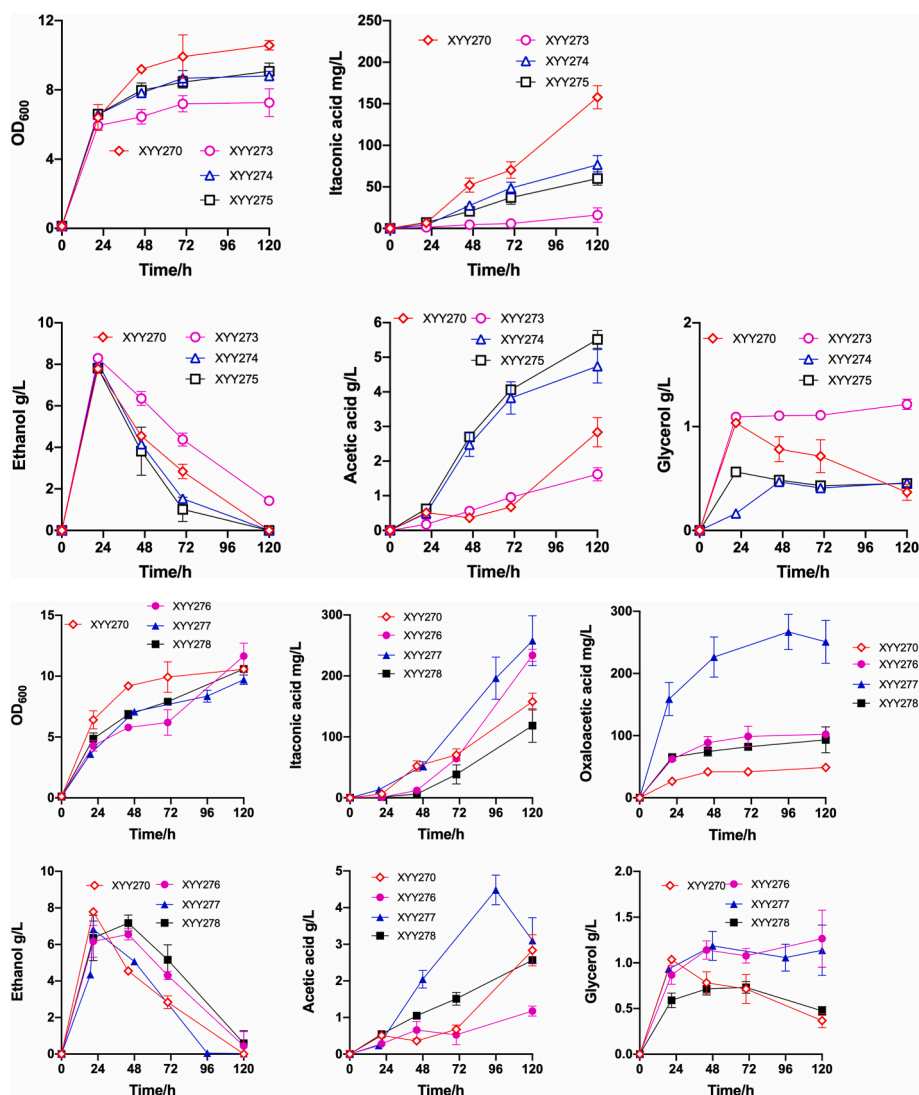


Fig. 3. Effect of enhanced acetate utilization on IA production and metabolism. (A) Effect of overexpression of ACKA-PTA on IA production. Profiles of cell density, IA, oxaloacetic acid, ethanol, acetic acid and glycerol concentrations in cultivation with YSCGLU medium with 20 g/L glucose. (B) Effect of overexpression of *Mt.acs* on IA production. Profiles of cell density, IA, oxaloacetic acid, ethanol, acetic acid and glycerol concentrations in cultivation with YSCGLU medium with 20 g/L glucose. The initial cell densities were approximately 0.1. The pH of the medium was adjusted with NaOH or HCl every 24 h to about 6.00. XYY270 (◇); XYY273 (○); XYY274 (△); XYY275 (□); XYY276 (●); XYY277 (▲); XYY278 (■). (C) Relative transcription levels of genes related to IA production in XYY271 and XYY277. The relative transcription levels of XYY271 at 48 h are indicated in blue; those of XYY277 are indicated in magenta. ACT1, actin; ALD4, mitochondrial acetaldehyde dehydrogenase; NDI1, mitochondrial internal NADH dehydrogenase; NDE1, mitochondrial external NADH dehydrogenase; SDH4, membrane anchor subunit of succinate dehydrogenase 4; QCR6, subunit 6 of the ubiquinol cytochrome-c reductase complex; QCR8, subunit 8 of ubiquinol cytochrome-c reductase (Complex III); QCR10, subunit of the ubiquinol-cytochrome c oxidoreductase complex; COX4, cytochrome oxidase subunit IV; COX6, Subunit VI of cytochrome c oxidase (Complex IV); ATP20, subunit g of the mitochondrial F1F0 ATP synthase; ATP14, subunit h of the F0 sector of mitochondrial F1F0 ATP synthase. The letters *, **, and *** above the bars indicate significant differences (*: $P < 0.05$, **: $P < 0.01$, and ***: $P < 0.001$).

synthesis.

It's reported phosphotransacetylase plays a role in the excretion of acetate by *E. coli* growing on glucose [33]. When *E. coli* grows on excess glucose or other carbon sources, up to 1/3 of the glucose could be excreted, mainly as acetate, via the reversible PTA-ACKA pathway [34]. The complete respiratory dissimilation of glucose in *S. cerevisiae* can produce 16 or 18 ATP. However, the fermentative pathway can only produce 2 ATP [35–37]. A lack of ATP during glucose fermentation may direct the reversible reaction of ACKA-PTA to acetic acid production. Although overexpression of *Mt.acs* sped up acetic acid utilization and IA formation, the impact was minimal. The above results showed that the

inability to meet the ATP demand of yeast for acetic acid utilization or glucose repression might be an important reason limiting the IA synthesis.

3.3. Activation of mitochondrial retrograde signaling improved acetic acid utilization and IA production

Amplification of the ethanol-acetyl-CoA pathway revealed that while ethanol-acetaldehyde consumption can provide cells with abundant NADH, it could be constrained by the cells' inability to oxidatively phosphorylate NADH, which is also a problem for acetate utilization.

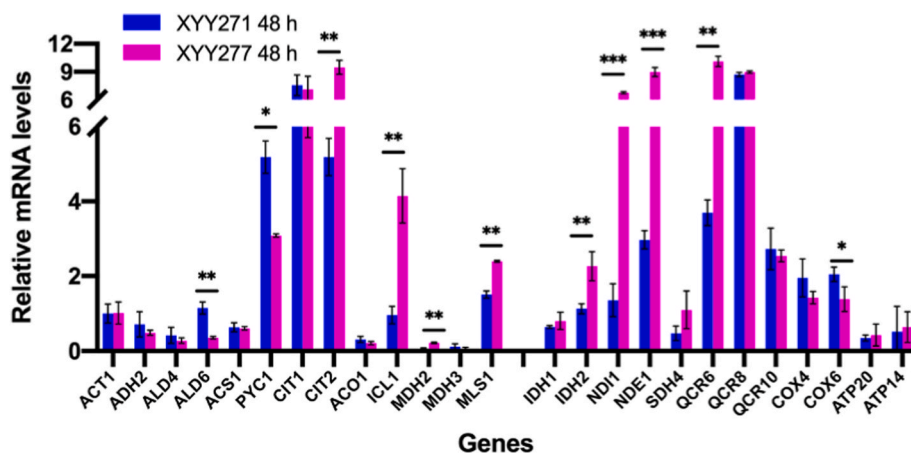


Fig. 3. (continued).

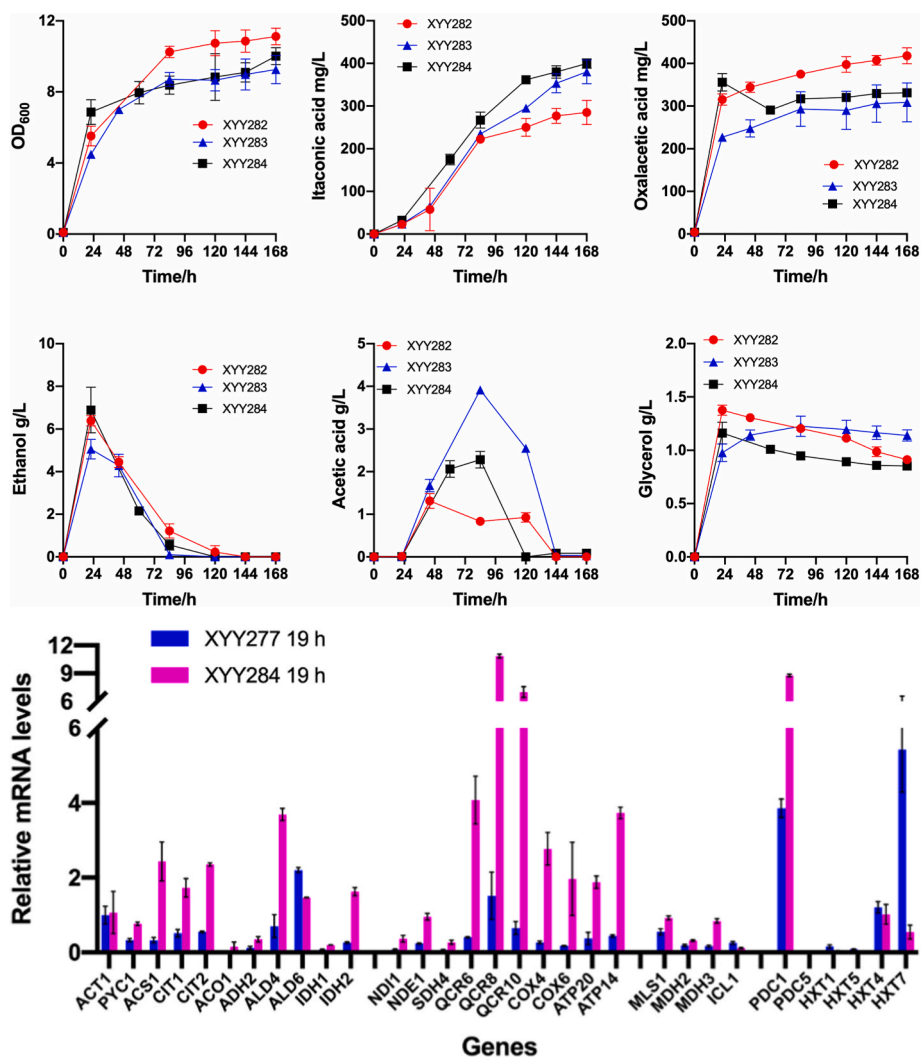


Fig. 4. Effect of enhanced RTG signal pathway on IA production and metabolism. (A) Effect of knockout of *mks1* on IA production and metabolism. Profiles of cell density, IA, oxaloacetic acid, ethanol, acetic acid and glycerol concentrations in cultivation with YSCGLU medium with 20 g/L glucose. XY282 (●); XY283 (▲); XY284 (■); *Mks1* was deleted in Strain XY282, XY283 and XY284. The initial cell densities were approximately 0.1. The pH of the medium was adjusted with NaOH or HCl every 24 h to about 6.00. (B) Relative transcription levels of genes related to IA production in XY277 and XY284. The relative transcription levels of XY277 at 19 h are indicated in blue; those of XY284 are indicated in magenta. PDC1, pyruvate decarboxylase; PDC5, pyruvate decarboxylase; HXT1, low-affinity glucose transporter of the major facilitator superfamily; HXT5, hexose transporter with moderate affinity for glucose; HXT4, high-affinity glucose transporter; HXT7, high-affinity glucose transporter. The results of the P value were not labeled on the picture.

Enhancing the TCA cycle helps to increase oxidative phosphorylation capacity [38,39]. The RTG signaling responds to intracellular changes in energy, including mitochondrial dysfunction. It activates the transcription of many nuclear genes encoding mitochondria on glucose, including those encoding the TCA cycle [15,16,40]. In addition, activating the RTG signaling not only promotes the production of ATP but also up-regulates the expression of target genes such as *pyc1*, *acs1*, *cit2* and *aco1* on glucose, which are all essential genes for IA production in the cytoplasm of *S. cerevisiae*. To relieve the inhibition of the RTG signaling by glucose, we knocked out the transcriptional repressor of the RTG signaling, MKS1, and performed flask shaking experiments [17,18]. Gene *mks1* in the strain *xyy270* was deleted, yielding strain *xyy282*; *mks1* in the strain *xyy271* was deleted, yielding strain *xyy283*; *mks1* in the strain *xyy277* was deleted, yielding strain *xyy284*.

As shown in Fig. 4A, the IA production rate of XYY282, XYY283 and XYY284 increased significantly, while IA production was advanced to the stage of glucose utilization (Fig. S4). The concentration of IA in XYY283 at 120 h in the supernatant improved from 207 mg/L to 295 mg/L. In the ethanol utilization stage, the concentration of acetic acid in XYY283 increased rapidly from 19 h to 84 h, and the rate of acetic acid consumption was faster after 84 h. Knockout of *mks1* contributed to the accelerated acetic acid utilization, as evidenced by the reduced acetic acid concentration in the supernatant of strain XYY282. In addition, *Mt.acs* was overexpressed based on strain XYY283. The titer of IA in XYY284 was further increased to 361 mg/L, the concentration of acetic acid in the supernatant was significantly lower than that of XYY283, and no acetic acid was detected in the supernatant at 120 h, which indicated that overexpressing *Mt.acs* and deleting *mks1* simultaneously further accelerated the utilization of acetic acid in *S. cerevisiae*.

qRT-PCR results in Fig. 4B showed that the relative expression levels of *cit1*, *aco1*, *idh1* and *idh2* at 19 h (Fig. S4, the stage of glucose utilization) in XYY284 were 3.3, 11.0, 2.5 and 6.2 times higher than those in XYY277, respectively. Furthermore, although the oxidative phosphorylation pathway is not a direct target of the RTG signaling, the relative expression levels of *ndi1*, *nde1*, *sdh4*, *qcr6*, *qcr8*, *qcr10*, *cox4*, *cox6*, *atp14* and *atp20* were 4.6, 4.0, 3.8, 8.4, 7.2, 10.7, 10.2, 11.3, 5.0 and 8.5 times higher than those of XYY277, respectively, which suggests that activating RTG signaling alleviates the glucose inhibition of the TCA cycle and respiratory chain pathways in *S. cerevisiae*. Besides, the relative expression levels of *pyc1*, *adh2*, *ald4*, *acs1*, *cit2* and *aco1* genes related to IA synthesis were 2.3, 2.9, 5.2, 7.4, 4.3 and 11.0 times higher than those of XYY277, respectively, which is consistent with the increased ethanol and acetic acid consumption and IA production.

3.4. Regulation of SNF1/MIG1 signaling improved oxidative phosphorylation pathway and IA production

Upregulating the mitochondrial TCA cycle and oxidative phosphorylation pathways is beneficial to improve ATP production. Through the overexpression of *Mt.acs* and the deletion of *mks1*, strain XYY284 improved IA production. Nevertheless, acetic acid remained in the supernatant for 19–84 h. To increase acetic acid utilization and respiratory capacity further, GSF2 and HXK2 related to the oxidative phosphorylation pathway were deleted, separately. Carbon catabolite repression is mediated, in part, by the crosstalk between two glucose signaling pathways: the RGT2/SNF3 axis responsible for glucose uptake; and the SNF1/MIG1 axis that negatively regulates the genes involved in respiratory metabolism and utilization of alternative sugars [34,35], which are two key regulators of glucose repression in *S. cerevisiae*. GSF2 is an integral membrane protein in the endoplasmic reticulum and involves the secretion of certain hexose transporters (such as HXT1) [22,41,42]. GSF2 was deleted in this paper since the functional link between the SNF1 signaling and GSF2 [23,34]. Strain *xyy290* was created by deleting *gsf2* from strain *xyy277*. Strain *xyy292* was created by deleting *gsf2* from strain *xyy284*.

Glycerol accumulation reflects whether cytoplasmic NADH exceeds

the capacity of mitochondrial oxidative phosphorylation, while ethanol secretion reflects whether mitochondrial NADH exceeds mitochondrial oxidative phosphorylation capacity [43]. Fig. 5A demonstrated that, after deletion of GSF2, the glycerol output of XYY290 decreased to 0.25 g/L drastically, which implied the oxidative phosphorylation ability of XYY290 may be strengthened during the glucose utilization stage. However, the IA production of strain XYY290 at 120 h dropped to 216 mg/L. The decreasing OAA may account for this. The combined deletion of MKS1 and GSF2 (XYY292) had little effect on glycerol production. Consequently, the IA production rate of XYY292 was slower than that of XYY284. Surprisingly, IA titer in XYY292 (493 mg/L) was higher than in XYY284 at 168 h, since XYY292 had accumulated more acetic acid than XYY284. Accordingly, acetyl-CoA and OAA, the two precursors for IA synthesis, should be distributed in a coordinated manner to maximize IA production.

The hexokinase HXK2, interacts with MIG1 (multicopy inhibitor of GAL gene expression) and influences glucose repression during glucose utilization. The respiratory pathway is improved when *hvk2* is knocked out [19]. Strain *xyy286* was created by deleting *hvk2* from strain *xyy277*. Strain *xyy288* was created by deleting *hvk2* from strain *xyy284*.

The production of IA in strain XYY288 did not change significantly, as shown in Fig. 5B. The biomass of the strain XYY286 increased during the phase of glucose utilization, and the production of IA enhanced significantly to 396 mg/L at 120 h and reached 535 mg/L at 168 h. Compared with the control strain XYY277, the IA production of the strain XYY286 increased by 54% at 120 h. The titer of OAA in XYY286 rose from 258 mg/L to 363 mg/L compared to the control strain XYY277 at 120 h. When *hvk2* was knocked out, BY4741 maintained the state of the Crabtree effect, in contrast to the outcomes of CEN.PK series yeast [21]. The difference in genetic backgrounds between the S288C and CEN.PK yeast may account for these variances [44]. As shown in Fig. 5C, the relative expression of the low-affinity glucose transporter protein HXT1, which is positively regulated by RGT2 signaling, was up-regulated by 3.3-fold, while the relative expression of the high-affinity glucose transporter proteins HXT4 and HXT7, which are negatively regulated by SNF1/MIG1 and SNF3 signaling, were down-regulated by 0.13-fold and 0.66-fold, respectively. Furthermore, the relative expression of the medium-affinity glucose transporter protein HXT5 was elevated 4.34-fold [45]. Considering the shake flask results, strain XYY286 consumed glucose faster than strain XYY277. These findings suggest there might be isozymes or other mechanisms to fill the gaps left by deleting the enzyme HXK2. Unexpectedly, qRT-PCR results revealed (Fig. 5C) that the relative expression of *cit1*, *aco1*, *idh1*, and *idh2* of the TCA cycle pathway of XYY286 was 4.4, 34.9, 3.0, and 5.9 times higher than that of XYY277, respectively. The relative expression of the genes *ndi1*, *nde1*, *sdh4*, *qcr6*, *qcr8*, *qcr10*, *cox4*, *cox6*, *atp20*, and *atp14* sampled for the oxidative phosphorylation pathway was, respectively, 3.3, 1.5, 5.6, 4.0, 9.0, 2.3, 6.4, 3.8, 3.5, and 4.7 times greater than that of XYY277. The differences were significant, indicating that *hvk2* knockout increased gene expressions related to mitochondrial respiration and metabolism, too. On the other hand, qRT-PCR results implied that *hvk2* deletion enhanced the precursor supply of acetyl-CoA and OAA. The relative expression of *pdh1* in XYY286 did not change, but *pdh5* had a 6.3-fold greater relative expression than XYY277. Combined with the increased titer of ethanol and acetic acid of XYY286 at 19 h, the metabolic flux of pyruvate decarboxylase was improved. Additionally, *icl1*, *mls1*, *mdh2*, *mdh3*, and *pyc1* had relative expression levels of 94.9, 229.4, 13.3, and 2.5 times greater than those of XYY277, respectively, which is consistent with enhanced OAA production during the phase of glucose utilization.

3.5. The upregulation of OAA synthesis pathway and pyruvate decarboxylase favors IA synthesis

Except for the difference in IA and acetic acid titers, XYY286 and XYY284 had increased OAA and IA titers significantly with the same

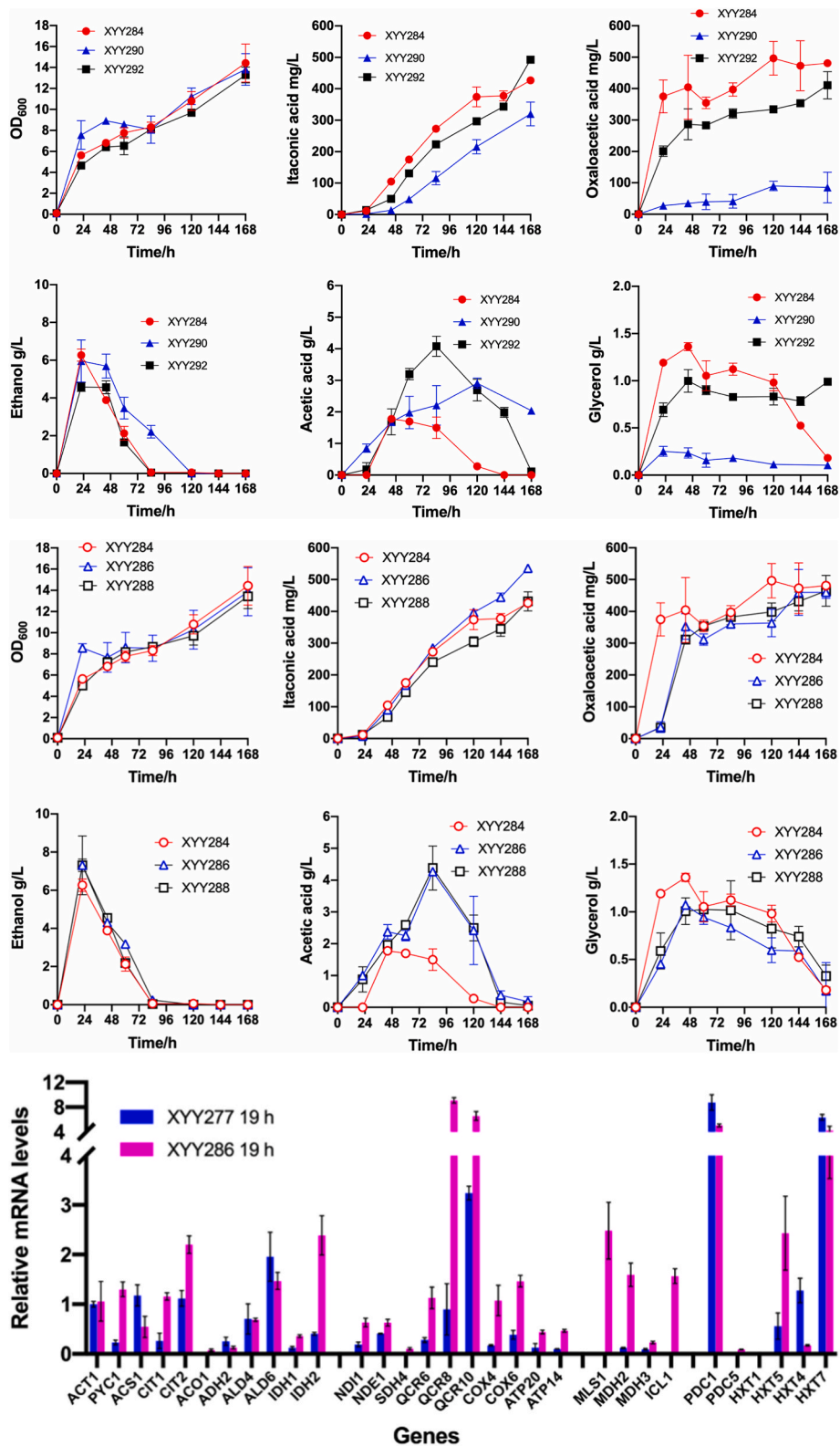


Fig. 5. Increasing the ATP supply through deletion of *gsf2* and *hxk2*. (A) Effect of deletion of *gsf2* on acetate utilization and IA production. Profiles of cell density, IA, oxaloacetic acid, ethanol, acetic acid and glycerol concentrations in cultivation with YSCGLU medium with 20 g/L glucose. XYY284 (●); XYY290 (▲); XYY292 (■); *Gsf2* was deleted in Strain XYY290 and XYY292. (B) Effect of knockout of *hxk2* on acetate utilization and IA production and metabolism. Profiles of cell density, IA, oxaloacetic acid, ethanol, acetic acid and glycerol concentrations in the cultivation of YSCGLU medium with 20 g/L glucose. XYY284 (○); XYY286 (△); XYY288 (□); *Hxk2* was deleted in Strain XYY286 and XYY288. The initial cell densities were approximately 0.1. The pH of the medium was adjusted with NaOH or HCl every 24 h to about 6.00. (C) Relative transcription levels of genes related to IA production in XYY277 and XYY286. The relative transcription levels of XYY277 at 19 h are indicated in blue; those of XYY286 are indicated in magenta. The results of the P value were not labeled on the picture. The initial cell densities were approximately 0.1. The pH of the medium was adjusted with NaOH or HCl every 24 h to about 6.00.

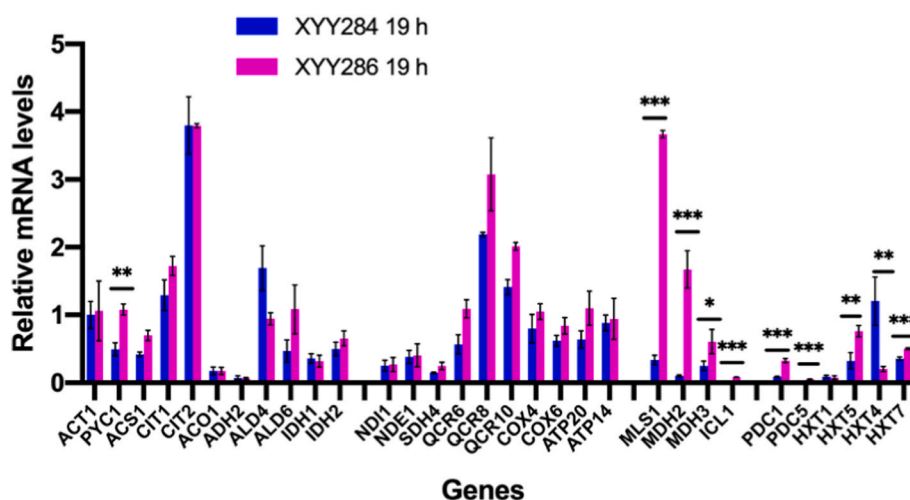


Fig. 6. (A) A glyoxylate pathway and pyruvate decarboxylase upregulation favors IA synthesis. Relative transcription levels of genes related to IA production in XYY286 and XYY288. The relative transcription levels of XYY286 at 19 h are indicated in blue; those of XYY288 are indicated in magenta. The letters *, **, and *** above the bars indicate significant differences (*: $P < 0.05$, **: $P < 0.01$, and ***: $P < 0.001$).

trend. qRT-PCR experiments were conducted to understand thoroughly why XYY286 produced more IA and acetic acid than XYY284. Fig. 6 demonstrated that the relative expression of *pyc1*, *icl1*, *mdh2*, and *mls1* in the cytoplasmic OAA synthesis pathway of XYY286 was 2.2, 7.4, 16.2, and 10.9 times greater than that of XYY284, respectively. The up-regulation of these genes strengthened the capacity of OAA synthesis of XYY286. Besides, the relative expression of the pyruvate dehydrogenases PDC1 and PDC5 was 3.7 and 2.5 times higher in XYY286 than in XYY284, respectively. There was a possibility that acetate accumulation in XYY286 could be caused by an increase in pyruvate directing to the ethanol-acetyl-CoA pathway. Fig. 5B showed that XYY286 accumulated more ethanol and acetic acid than XYY284 at 19 h. The metabolic flow of the ethanol-acetyl-CoA pathway was driven by the up-regulated expression of pyruvate decarboxylase. In summary, IA production was improved by the enhanced expression of the OAA synthesis pathway and pyruvate decarboxylase, and more NADH was available for OAA synthesis catalyzed by MDH2 in the glyoxylate pathway.

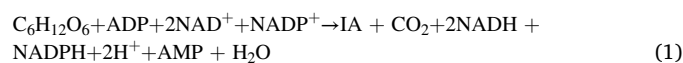
4. Discussion

As an important organic acid compound, IA is a notable monomer for many valuable biological products. IA is primarily produced by the TCA cycle and glyoxylate pathway. However, the Crabtree effect of *S. cerevisiae* limits the metabolic flow of the citrate synthesis pathway, and engineered Crabtree-negative strains always sacrifice strain growth in glucose medium to increase the metabolic flux of these pathways. The two-stage production of IA with glucose as a substrate is more suitable for Crabtree-positive yeasts. Previously, an IA synthesis pathway in the cytoplasm of *S. cerevisiae* was designed and synthesized, and complex optimization and modification of the metabolic pathway were carried out to increase the production of cytoplasmic IA [9]. We performed another efficient method to activate IA synthesis and oxidative phosphorylation pathways by rewiring signaling pathways. By improving precursors acetyl-CoA, OAA, and energy supply, IA production was finally boosted to 535 mg/L.

Energy regulation has been an issue non-ignorable when modifying the cytoplasmic IA synthesis pathway, and promoting the TCA cycle and oxidative phosphorylation contribute to the energy supply for synthesizing precursor OAA and acetyl-CoA. Urea has more advantages over ammonium sulfate as a nitrogen source, including alkalizing cytoplasmic pH and providing CO_2 for OAA synthesis. The supply-demand relationship of ATP and NADH between urea uptake and Dz.ADA

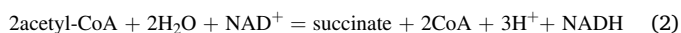
reaction may be one reason for the increased production of IA in the urea medium when Dz.ADA was overexpressed. However, the results of ACKA-PTA and Mt.ACS overexpression revealed that a lack of cytoplasmic ATP may limit the precursor supply. Increasing the TCA cycle and oxidative phosphorylation is a valuable strategy for boosting ATP levels. Our experiments demonstrated that transcriptional activators related to glucose sensing and signaling mechanisms are feasible and effective targets. Instead of expressing genes of the IA synthesis pathway, MKS1, a transcriptional repressor of the RTG signaling, was knocked out directly. Which strengthened the TCA cycle and oxidative phosphorylation pathways through metabolic regulation, increased the rate of acetate utilization, and the up-regulated expression of cytoplasmic IA synthesis pathway genes *pyc1*, *cit2*, *aco1* and others were beneficial to increasing IA production. Similar to the effect of ΔMKS1 , ΔHXX2 up-regulated the TCA cycle and oxidative phosphorylation pathways and increased the supply of acetyl-CoA and OAA, too. The difference is that the relative expression levels of the downstream genes of the glyoxylate pathway: *icl1*, *mls1* and *mdh2* were up-regulated further, and more NADH was provided in XYY286 than in XYY284. The similar effects between XYY284 and XYY286 may be because the RTG signaling is activated by the transcription factors ADR1 and CAT8, which are inhibited by the SNF1/MIG1 signaling as well [20]. Because of this crosstalk between the signaling pathways and related targets, although the regulated signaling pathways are distinct, the characterizations of the generated strains are comparable. The impacts of ΔHXX2 on the respiratory and glyoxylate pathways are still crucial for enhancing the generation of IA, even though they were unable to alleviate the Crabtree effect in XYY286 as the CEN.PK series could.

Shack flask results of strain XYY286 at 168 h showed that 33.01% of glucose was converted to OAA and pyruvate remained in the medium, and about 26.64% of glucose was used for yeast growth, a total of 3.75%–7.5% of glucose was converted to IA. The IA yield from total consumed glucose was 2.65% in *S. cerevisiae* XYY286 (Table S2). The increased OAA and pyruvate during 19–168 h implied OAA was not a limited precursor for IA production. If the cytoplasmic glyoxylate pathway (excluding MDH2) and pyruvate carboxylase account for all of the IA production, then only 3.75% of glucose is used for IA production. The reaction equation for IA production from glucose through the cytoplasmic glyoxylate pathway is as follows:



Due to lacking the complex I-type NADH dehydrogenases in

S. cerevisiae, the complete respiratory dissimilation of glucose yields approximately 16 or 18 ATP per glucose [35–37]. By hydrolyzing one ATP, Pma1p pumps $3H^+$ out of the cell. The reactions above show that IA production is generally a process of energy excess, and the flux of OAA and acetyl-CoA supplied pathways in the cytoplasm is enough for higher IA production. However, little glucose was used for IA production. Acetic acid absorption of XYY284 and XYY286 in Fig. 5B implied that insufficient acetic acid supply limited IA production. These results suggest that there could be an overflow of acetyl-CoA that limits IA production. Fatty acid synthesis could be one of the exports, as evidenced by recent studies on isotopic labeling [20]. The synthesis of succinate by the glyoxylate pathway and its entry into the mitochondria could be another cause of the acetyl-CoA loss. The following reaction equation showed that two molecules of acetyl-CoA are transferred to one molecule of succinate. These reactions are catalyzed by the enzymes CIT2, ACO1, ICL1, MLS1, and MDH2:



By the way, more work is needed to confirm whether the enzymatic activities of citrate synthase, aconitase, and *cis*-aconitate decarboxylase limit IA synthesis [11,46,47].

In conclusion, we increased IA titer by reducing some signaling pathways related to glucose repression, which upregulated the gene expressions of the IA synthesis and respiratory pathways during the growth on glucose. However, more specific work is needed to reduce the metabolic overflow of acetyl-CoA. Bypassing the ethanol-acetyl-CoA pathway and creating acetyl-CoA directly by overexpressing the pyruvate dehydrogenase (PDH) complex is another possible way of acetyl-CoA production and avoiding toxic intermediates accumulation. However, the redox balance during glucose utilization is a concern. Metabolic regulation of the glucose-sensing signaling pathway effectively increases gene expressions related to glucose derepression, which provides a reference for other studies linked to the Crabtree-positive phenotype.

CRedit authorship contribution statement

Yaying Xu: Conceptualization, Investigation, Formal analysis, Writing – original draft, Writing – review & editing. **Zhimin Li:** Conceptualization, Writing – review & editing, Supervision.

Declaration of competing interest

The authors declare that they have no competing interests.

Acknowledgments

Support for this study was provided by the China National Key Research and Development Program [2019YFA0904300].

Appendix A. Supplementary data

Supplementary data to this article can be found online at <https://doi.org/10.1016/j.synbio.2022.12.007>.

References

- Cornejo-Bravo JM, Palomino K, Palomino-Vizcaino G, Pérez-Landeros OM, Curiel-Alvarez M, Valdez-Salas B, Bucio E, Magaña H. Poly(n-vinylcaprolactam) and salicylic acid polymeric prodrug grafted onto medical silicone to obtain a novel thermo- and ph-responsive drug delivery system for potential medical devices. *Materials* 2021;14(5):1065. <https://doi.org/10.3390/ma14051065>.
- Sutthiwanjampa C, Shin BH, Ryu NE, Kang SH, Heo CY, Park H. Assessment of human adipose-derived stem cell on surface-modified silicone implant to reduce capsular contracture formation. *Bioeng. Transl. Med.* 2022;7(1):e10260. <https://doi.org/10.1002/btm2.10260>.
- Dan CV. Recent advances in biotechnological itaconic acid production, and application for a sustainable approach. *Polymers* 2021;13(20):3574. <https://doi.org/10.3390/polym13203574>.
- Krull S, Hevekerl A, Kuenz A, Prüße U. Process development of itaconic acid production by a natural wild type strain of aspergillus terreus to reach industrially relevant final titers. *Appl Microbiol Biotechnol* 2017;101(10):4063–72. <https://doi.org/10.1007/s00253-017-8192-x>.
- Hossain AH, Ter Beek A, Punt PJ. Itaconic acid degradation in aspergillus Niger: the role of unexpected bioconversion pathways. *Fungal Biol. Biotechnol.* 2019;6(1):1. <https://doi.org/10.1186/s40694-018-0062-5>.
- Harder BJ, Bettenbrock K, Klant S. Temperature-dependent dynamic control of the tea cycle increases volumetric productivity of itaconic acid production by escherichia coli. *Biotechnol Bioeng* 2018;115(1):156–64. <https://doi.org/10.1002/bit.26446>.
- Bafana R, Pandey RA. New approaches for itaconic acid production: bottlenecks and possible remedies. *Crit Rev Biotechnol* 2018;38(1):1–15. <https://doi.org/10.1080/07388551.2017.1312268>.
- Becker J, Tehrani HH, Ernst P, Blank LM, Wierckx N. An optimized ustilago maydis for itaconic acid production at maximal theoretical yield. *J. Fungi* 2020;7(1):20. <https://doi.org/10.3390/jof701020>.
- Young EM, Zhao Z, Gielesen BEM, Wu L, Gordon DB, Roubos JA, Voigt CA. Iterative algorithm-guided design of massive strain libraries, applied to itaconic acid production in yeast. *Metab Eng* 2018;48:33–43. <https://doi.org/10.1016/j.ymben.2018.05.002>.
- Blazcek J, Miller J, Pan A, Gengler J, Holden C, Jamoussi M, Alper HS. Metabolic engineering of saccharomyces cerevisiae for itaconic acid production. *Appl Microbiol Biotechnol* 2014;98(19):8155–64. <https://doi.org/10.1007/s00253-014-5895-0>.
- Xu Y, Li Z. Utilization of ethanol for itaconic acid biosynthesis by engineered saccharomyces cerevisiae. *FEMS Yeast Res* 2021;21(6). <https://doi.org/10.1093/femsyr/foab043>.
- Xiao T, Khan A, Shen Y, Chen L, Rabinowitz JD. Glucose feeds the tricarboxylic acid cycle via excreted ethanol in fermenting yeast. *Nat Chem Biol* 2022:1–8. <https://doi.org/10.1038/s41589-022-01091-7>.
- Liu Y, Bai C, Liu Q, Xu Q, Qian Z, Peng Q, Yu J, Xu M, Zhou X, Zhang Y, Cai M. Engineered ethanol-driven biosynthetic system for improving production of acetyl-coa derived drugs in crabtree-negative yeast. *Metab Eng* 2019;54:275–84. <https://doi.org/10.1016/j.ymben.2019.05.001>.
- Meadows AL, Hawkins KM, Tsegaye Y, Antipov E, Kim Y, Raetz L, Dahl RH, Tai A, Mahatdejkul-Meadows T, Xu L, Zhao L, Dasika MS, Murarka A, Lenihan J, Eng D, Leng JS, Liu C-L, Wenger JW, Jiang H, Chao L, Westfall P, Lai J, Ganesan S, Jackson P, Mans R, Platt P, Reeves CD, Saija PR, Wichmann G, Holmes VF, Benjamin K, Hill PW, Gardner TS, Tsong AE. Rewriting yeast central carbon metabolism for industrial isoprenoid production. *Nature* 2016;537(7622):694–7. <https://doi.org/10.1038/nature19769>.
- Hashim Z, Mukai Y, Bamba T, Fukusaki E. Metabolic profiling of retrograde pathway transcription factors rtg1 and rtg3 knockout yeast. *Metabolites* 2014;4(3):580–98. <https://doi.org/10.3390/metabo4030580>.
- Plocek V, Fadrhonic K, Maršiková J, Váňková L, Pokorná A, Hlaváček O, Wilkinson D, Palková Z. Mitochondrial retrograde signaling contributes to metabolic differentiation in yeast colonies. *Int J Mol Sci* 2021;22(11):5597. <https://doi.org/10.3390/ijms22115597>.
- Schüller H-J. Transcriptional control of nonfermentative metabolism in the yeast saccharomyces cerevisiae. *Curr Genet* 2003;43(3):139–60. <https://doi.org/10.1007/s00294-003-0381-8>.
- Sekito T, Liu Z, Thornton J, Butow RA. Rtg-dependent mitochondria-to-nucleus signaling is regulated by mks1 and is linked to formation of yeast prion [ure3]. *Mol Biol Cell* 2002;13(3):795–804. <https://doi.org/10.1091/mbc.01-09-0473>.
- Diderich JA, Raamsdonk LM, Kruckeberg AL, Berden JA, Van Dam K. Physiological properties of saccharomyces cerevisiae from which hexokinase ii has been deleted. *Appl Environ Microbiol* 2001;67(4):1587–93. <https://doi.org/10.1128/aem.67.4.1587-1593.2001>.
- Laera L, Guaragnella N, Ždravlević M, Marzulli D, Liu Z, Giannattasio S. The transcription factors adr1 or cat8 are required for rtg pathway activation and evasion from yeast acetic acid-induced programmed cell death in raffinose. *Microbial Cell* 2016;3(12):621–31. <https://doi.org/10.15698/mic2016.12.549>.
- Schuermans JM, Boorsma A, Lascaris R, Hellingwerf KJ, Teixeira de Mattos MJ. Physiological and transcriptional characterization of saccharomyces cerevisiae strains with modified expression of catabolic regulators. *FEMS Yeast Res* 2008;8(1):26–34. <https://doi.org/10.1111/j.1567-1364.2007.00309.x>.
- Sherwood PW, Carlson M. Mutations in gsf1 and gsf2 alter glucose signaling in saccharomyces cerevisiae. *Genetics* 1997;147(2):557–66. <https://doi.org/10.1093/genetics/147.2.557>.
- Baek S-H, Kwon EY, Kim S-Y, Hahn J-S. Gsf2 deletion increases lactic acid production by alleviating glucose repression in saccharomyces cerevisiae. *Sci Rep* 2016;6(1):34812. <https://doi.org/10.1038/srep34812>.
- Zhang G-C, Kong II, Kim H, Liu J-J, Cate JHD, Jin Y-S. Construction of a quadruple auxotrophic mutant of an industrial polyplid saccharomyces cerevisiae strain by using rna-guided cas9 nuclease. *Appl Environ Microbiol* 2014;80(24):7694–701. <https://doi.org/10.1128/aem.02310-14>.
- Haber JE. In vivo biochemistry: physical monitoring of recombination induced by site-specific endonucleases. *Bioessays* 1995;17(7):609–20. <https://doi.org/10.1002/bies.950170707>.
- Reider Apel A, d'Espaux L, Wehrs M, Sachs D, Li RA, Tong GJ, Garber M, Nnadi O, Zhuang W, Hillson NJ, Keasling JD, Mukhopadhyay A. A cas9-based toolkit to

- program gene expression in *saccharomyces cerevisiae*. *Nucleic Acids Res* 2017;45(1):496–508. <https://doi.org/10.1093/nar/gkw1023>.
- [27] Huang B, Yang H, Fang G, Zhang X, Wu H, Li Z, Ye Q. Central pathway engineering for enhanced succinate biosynthesis from acetate in *escherichia coli*. *Biotechnol Bioeng* 2018;115(4):943–54. <https://doi.org/10.1002/bit.26528>.
- [28] Sun L, Lee JW, Yook S, Lane S, Sun Z, Kim SR, Jin Y-S. Complete and efficient conversion of plant cell wall hemicellulose into high-value bioproducts by engineered yeast. *Nat Commun* 2021;12(1):4975. <https://doi.org/10.1038/s41467-021-25241-y>.
- [29] van den Berg MA, de Jong-Gubbels P, Kortland CJ, van Dijken JP, Pronk JT, Steensma HY. The two acetyl-coenzyme a synthetases of *saccharomyces cerevisiae* differ with respect to kinetic properties and transcriptional regulation. *J Biol Chem* 1996;271(46):28953–9. <https://doi.org/10.1074/jbc.271.46.28953>.
- [30] Berger S, Welte C, Deppenmeier U. Acetate activation in *methanoseta thermophila*: characterization of the key enzymes pyrophosphatase and acetyl-coa synthetase. *Archaea-an International Microbiological Journal* 2013;2012(1):315153. <https://doi.org/10.1155/2012/315153>.
- [31] Meng Y, Ingram-Smith C, Cooper LL, Smith KS. Characterization of an archaeal medium-chain acyl coenzyme a synthetase from *methanosarcina acetivorans*. *J Bacteriol* 2010;192(22):5982–90. <https://doi.org/10.1128/jb.00600-10>.
- [32] El-Mansi EMT, Holms WH. Control of carbon flux to acetate excretion during growth of *escherichia coli* in batch and continuous cultures. *Microbiology* 1989;135(11):2875–83. <https://doi.org/10.1099/00221287-135-11-2875>.
- [33] Brown TDK, Jones-Mortimer MC, Kornberg HL. The enzymic interconversion of acetate and acetyl-coenzyme a in *escherichia coli*. *Microbiology* 1977;102(2):327–36. <https://doi.org/10.1099/00221287-102-2-327>.
- [34] Kern A, Tilley E, Hunter IS, Legi AM, Glieder A. Engineering primary metabolic pathways of industrial micro-organisms. *J Biotechnol* 2007;129(1):6–29. <https://doi.org/10.1016/j.jbiotec.2006.11.021>.
- [35] Vries SD, Marres C. The mitochondrial respiratory chain of yeast. Structure and biosynthesis and the role in cellular metabolism. *Biochim Biophys Acta Rev Bioenerg* 1987;895(3):205–39. [https://doi.org/10.1016/S0304-4173\(87\)80003-4](https://doi.org/10.1016/S0304-4173(87)80003-4).
- [36] Cornelis Verduyn, Adriaan H, Stouthamer W, Alexander, Scheffers Johannes P, Dijken. A theoretical evaluation of growth yields of yeasts. *Antonie Leeuwenhoek* 1991;59:49–63. <https://doi.org/10.1007/BF00582119>.
- [37] van Gulik WM, Heijnen JJ. A metabolic network stoichiometry analysis of microbial growth and product formation. *Biotechnol Bioeng* 1995;48(6):681–98. <https://doi.org/10.1002/bit.260480617>.
- [38] Yin X, Li J, Shin H-d, Du G, Liu L, Chen J. Metabolic engineering in the biotechnological production of organic acids in the tricarboxylic acid cycle of microorganisms: advances and prospects. *Biotechnol Adv* 2015;33(6):830–41. <https://doi.org/10.1016/j.biotechadv.2015.04.006>.
- [39] Vuoristo KS, Mars AE, Sanders JPM, Eggink G, Weusthuis RA. Metabolic engineering of tca cycle for production of chemicals. *Trends Biotechnol* 2016;34(3):191–7. <https://doi.org/10.1016/j.tibtech.2015.11.002>.
- [40] Zhang F, Pracheil T, Thornton J, Liu Z. Adenosine triphosphate (atp) is a candidate signaling molecule in the mitochondria-to-nucleus retrograde response pathway. *Genes* 2013;4(1):86–100. <https://doi.org/10.3390/genes4010086>.
- [41] Sherwood PW, Carlson M. Efficient export of the glucose transporter hxt1p from the endoplasmic reticulum requires gsf2p. *Proc Natl Acad Sci U S A* 1999;96(13):7415–20. <https://doi.org/10.1073/pnas.96.13.7415>.
- [42] Kota J, Ljungdahl PO. Specialized membrane-localized chaperones prevent aggregation of polytopic proteins in the er. *J Cell Biol* 2005;168(1):79–88. <https://doi.org/10.1083/jcb.200408106>.
- [43] Vemuri GN, Eiteman MA, McEwen JE, Olsson L, Nielsen J. Increasing nadh oxidation reduces overflow metabolism in *saccharomyces cerevisiae*. *Proc Natl Acad Sci U S A* 2007;104(7):2402–7. <https://doi.org/10.1073/pnas.0607469104>.
- [44] Kümmel A, Ewald JC, Fendt SM, Jol SJ, Picotti P, Aebersold R, Sauer U, Zamboni N, Heinemann M. Differential glucose repression in common yeast strains in response to hxx2 deletion. *FEMS Yeast Res* 2010;10(3):322–32. <https://doi.org/10.1111/j.1567-1364.2010.00609.x>.
- [45] Rolland F, Winderickx J, Thevelein JM. Glucose-sensing and -signalling mechanisms in yeast. *FEMS Yeast Res* 2002;2(2):183–201. <https://doi.org/10.1111/j.1567-1364.2002.tb00084.x>.
- [46] Kispal G, Srere PA. Studies on yeast peroxisomal citrate synthase. *Arch Biochem Biophys* 1991;286(1):132–7. [https://doi.org/10.1016/0003-9861\(91\)90018-E](https://doi.org/10.1016/0003-9861(91)90018-E).
- [47] Dwiarti L, Yamane K, Yamatani H, Kahar P, Okabe M. Purification and characterization of cis-aconitic acid decarboxylase from *aspergillus terreus* tn484-m1. *J Biosci Bioeng* 2002;94(1):29–33. [https://doi.org/10.1016/s1389-1723\(02\)80112-8](https://doi.org/10.1016/s1389-1723(02)80112-8).